Numerical simulations of the oxygen impurity transport at the plasma periphery in a Tokamak

J. Neuhauser, M. Tendler*),
R. Wunderlich

IPP 1/221 October 1983

MAX-PLANCK-INSTITUT FÜR PLASMAPHYSIK
8046 GARCHING BEI MÜNCHEN

MAX-PLANCK-INSTITUT FÜR PLASMAPHYSIK

GARCHING BEI MÜNCHEN

Numerical simulations of the oxygen impurity transport at the plasma periphery in a Tokamak

J. Neuhauser, M. Tendler*),
R. Wunderlich

IPP 1/221 October 1983

*) Royal Institute of Technology, Stockholm, Sweden

Die nachstehende Arbeit wurde im Rahmen des Vertrages zwischen dem Max-Planck-Institut für Plasmaphysik und der Europäischen Atomgemeinschaft über die Zusammenarbeit auf dem Gebiete der Plasmaphysik durchgeführt.

Numerical simulations of the oxygen impurity transport at the plasma periphery in a Tokomak.

M. Tendler, Royal Institute of Technology, Stockholm, Sweden

and

J. Neuhauser, R. Wunderlich, Max-Planck- Institut für Plasmaphysik, Euratom Association, D-8046 Garching, Germany.

Abstract

The behaviour of oxygen, which is one of the most frequently encountered impurity species in tokomaks, is particularly complicated owing to the intensive cross charge exchange processes between oxygen and hydrogen. Another complication arises from the fact that oxygen is desorbed from metallic surfaces as hydrogenic or metallic compounds, undergoing a sophisticated multistep evolution before arriving at the neutral atomic state. Here we study the influence of these effects, using the numerical algorithm, which allows fast solution of both the steady-state and the time-dependent one-dimensional-finite rate diffusion equations [1]. The auxiliary calculations, accounting for the cross charge exchange and the sub-routine describing the low energy chemical kinetics, are incorporated in the code.

I. Introduction

At present, the computer modelling of impurity behaviour in tokomaks is hampered by gaps still left in our knowledge of impurity transport, scrape-off physics and the plasma-wall interaction. Improved understanding of these issues should allow one to obtain a comprehensive and self-consistent model suitable for asessing the physics of the impurity transport at the plasma periphery in all its complexity.

Radiative cooling of the plasma by impurities is an effect which can range from devastating to beneficial, depending on the location of the ionization states of impurities and their radiative cooling parameters. Strong cooling of the plasma core via line radiation from the low ionization states of heavy metals reduces the confinement and might prevent fusion from taking place.

On the other hand, a scenario has been suggested, which relies upon the gradual build-up of the intensely radiating impurities in the edge region, thus channelling the significant part of the energy flux from the plasma interior into the boundary radiation [1,2]. This scheme offers the possibility of reducing the heat flux onto the limiter and of protecting the limiter from thermal overloading.

The charge state of the impurity ion, which is reached before it arrives at the boundary surface, has a powerful effect upon the surface erosion sputtering. This effect is important because the initially neutral impurity atom gets ionized and returns to the surface with the energy significantly increased after acceleration through the plasma sheath. The energy gain is a strong function of the ionic charge.

The study of the impurity transport is also of particular interest at the plasma periphery owing to the usually invoked arguments that the excessive boundary radiation may lead to disruptions or lower the empirical density limit [3].

To assess the issue, the overall density of impurities and their distribution over the ionization states at the periphery have to be precisely known. Recently, the algorithm allowing fast solution of both the steady and the time dependent one dimensional finite rate diffusion equations was developed [4]. It allows one to follow the gradual evolution of the impurity distribution over the ionization states both in time and space.

The one-dimensional transport model, which is found to fit ASDEX experimental results was applied to impurity species with different ionic charge.

In this calculations neutral impurity density distribution was arbitrarily prescribed by a source, sharply peaked in the vicinity of the metallic surface.

The problem, not treated there, concerns the effect of the impurity neutral penetration mechanism on the impurity transport in the edge region of a tokomak. This issue is particularly complicated for oxygen, which is the most common intrinsic impurity, owing to the intensive cross charge exchange processes between oxygen and hydrogen. In a number of the recent publications on the impurity transport the case of oxygen has been either explicitly excluded owing to the difficulty in accounting for the cross charge exchange processes [5] or simulated by varying the effective neutral oxygen atom velocity [6].

The other complication arises from the fact that oxygen is desorbed from the metallic surfaces as hydrogenic or metallic compounds, thus passing through a sophisticated multistep evolution before arriving at the neutral atomic state. In [7] it was shown that both the penetration of the neutral oxygen and the effective diffusion coefficient of the singly ionized oxygen ion are significantly enhanced owing to the cross charge exchange processes The variety of chemical processes, important to oxygen transport, includes ionization of the oxygen atoms by the electron and proton impact, dissociation of the neutral molecular compounds, and collisional dissociation, dissociative recombination and kinetic energy transfer by protons for the molecular oxygen ions. Here, we have neglected the transport of the molecular ions across field lines, assuming that the destruction of these ions occur much faster than the transport across the magnetic field. The influence of vibrational excitation of edge molecules on the branching ratios of the chemical processes has also been neglected [8].

In the present paper, we study the influence of these effects on the oxygen ion transport explicitly using auxiliary calculations described in [7] in addition to the numerical algorithm [4], as part of our physical model, accounting for the charge exchange processes between a proton and a neutral oxygen atom and a neutral hydrogen atom with a singly ionized oxygen ion. A subroutine describing the kinetics of the typical oxygen molecular compound is also incorporated in our code.

The emphasis here is on elucidating the differences between the oxygen and the other types of impurities. The analysis indicates that there are qualitative and quantitative differences in transport of oxygen at the periphery. The peculiarities of the atomic and molecular processes for oxygen are found to be very important for the transport of the atomic and molecular ions. The most significant differences in the transport are:
a) the total impurity content in the plasma increases due to the significant enhancement of the penetration depth of oxygen atoms and
b) the recycling of the singly ionized atomic ions at the wall is more efficient in the presence of the cross charge exchange processes between oxygen and hydrogen.

2. Transport model

For each of the oxygen species with the charge Z the following flux surface averaged continuity equations hold:

$$\frac{\partial n_z}{\partial t} + \frac{1}{r}\frac{\partial}{\partial r}(r\Gamma_z) = n_e\left[n_{z-1}S_{z-1} - n_z S_z + n_{z+1}\alpha^{r.d}_{z+1} - n_z\alpha^{r.d}_z\right] - \frac{n_z}{\tau_{II}} \quad \text{for } z \geq 2 \tag{2.1}$$

$$\frac{\partial n_1}{\partial t} + \frac{1}{r}\frac{\partial}{\partial r}(r\Gamma_1) = n_e\left[n_o S_o - n_1 S_1\right] + C_{01}n_i n_o - C_{10}n_1 n_H - \frac{n_1}{\tau_{II}} \tag{2.2}$$

$$\frac{\partial n_o}{\partial t} - \frac{1}{r}\frac{\partial}{\partial r}(r\Gamma_o) = -n_e n_o S_o - C_{01}n_i n_o + C_{10}n_1 n_H + S_M(r) \tag{2.3}$$

Here, n_z are the densities of the oxygen ions of charge Z, S_z are the ionization rate coefficients, and $\alpha^{r.d}_z$ are the recombination (radiative plus dielectronic) rate coefficients. For the lower ionization states the recombination is a very small effect and can be neglected. C_{01} and C_{10} are the charge exchange rates for cross charge exchange $O+H^+ \rightarrow O^+ + H$, $O^+ + H \rightarrow O + H^+$, respectively. S_M stands for the neutral atomic oxygen source, resulting from the impurities desorbed as molecular compounds.
The incorporation of these effects constitutes the basic difference between our treatment and the previous studies [4,6] The terms $-\frac{n_z}{\tau_{II}}$ are added to simulate a loss to a limiter or to divertor plates in the scrape-off layer. Finally, Γ_z is the radial particle flux density, which is taken to be positive when directed outwards. It is assumed here to conform to the scaling found to fit the results from ASDEX [9]:

$$\Gamma_z = -D\frac{dn_z}{dr} + v_D n_z \tag{2.4}$$

In the following, D is taken to be spatially independent and of the order $4 \times 10^3 cm^2 sec^{-1}$. The inward term is smaller at the periphery due to the steep gradient and is neglected. n_o and S_M are used in the form obtained in [7]. The system of equations (2.1) - (2.4) can be solved numerically if the plasma, the neutral hydrogen density and the plasma temperature profiles are given.

In the equations (2.2) - (2.3) the new terms introduce additional coupling and a new source. From equation (2.3) it follows that the ionization of the oxygen neutrals is quite large even at a very low electron temperature, when the ionization rate by the electron impact is negligible, owing to the charge exchange with protons.

3. Analytical solution for the model equation in the scrape-off layer.

Summing up an arbitrary number of equations of the system (2.1)-(2.3) (i.e. up to a certain value of Z) it is easily seen that the equation, describing the total flux of the arbitrary sum over the ionization states will contain only the source of the lowest ionization term and a sink equal to the sink of the largest Z, plus the total parallel loss. The interchange terms cancel.

This simple observation allows separation of certain ionization states into the blocks (i.e. $0 \leqslant Z \leqslant 5$ and $Z > 5$), which under some conditions might be treated independently. For example, the sum of the low ionization states ($0 \leqslant Z \leqslant 5$) can be decoupled from the higher ionization states, if the parallel losses to the target plates significantly exceed the sink to the next ionization state. This scheme, applied to the overall amount of species with the same diffusion coefficient, was used in [10] for heavy impurities. The flux of the impurity neutrals was assumed to be purely convective and the influence of the scrape-off layer was neglected. The steady state model equation in the plane geometry for the total number of ions in the block takes the form

$$-D \frac{d^2N}{dx^2} = n_e n_o S_o + C_{01} n_i n_o - C_{10} n_i n_H - n_e n_n S_n + n_e n_{n+1} \alpha_{n+1} - \frac{N}{\tau_{\parallel}} \qquad (3.1)$$

Here, $N = \sum_{z=1}^{n} n_z$, where 1 and n are the lowest and the highest ionization states in the block. Neglecting the recombination and the ionization to and from the highest ionization state and introducing the source function S, equal to the sum of the first three terms on the r.h.s. of eq. (3.1), we get

$$-D \frac{d^2N}{dx^2} = S - \frac{N}{\tau_{\parallel}} \qquad (3.2)$$

In solving the transport equation (3.2) the following boundary conditions have been used:

$$N\Big|_{x=0} = 0 \tag{3.3a}$$

$$D\,\frac{dN}{dx}\Big|_{x=0} + \int_0^a \frac{N}{\tau}\,dx = \Gamma_o \tag{3.3b}$$

where a is the distance from the limiter head to the wall , x is equal to zero at the wall and Γ_o is the influx of the impurity neutrals at x=0.

Equation (3.2) can be solved analytically for an arbitrary source term. The solution of equation (3.2) reads:

$$N = C_1 \exp(\tfrac{x}{\lambda}) + C_2 \exp(-\tfrac{x}{\lambda}) - \exp(\tfrac{x}{\lambda}) \int_0^x \exp(-\tfrac{x}{\lambda})\, x\, S\, \frac{\lambda}{2}\,dx + \exp(-\tfrac{x}{\lambda}) \int_0^x \exp(\tfrac{x}{\lambda})\, S\, \frac{\lambda}{2}\,dx \tag{3.4}$$

where $\lambda = \sqrt{D\tau_{\parallel}}$ is the decay length of impurities in the scrape-off layer.

As an example, we take the model source function as:

$$S = S_o \exp\left[-x(\tfrac{1}{\delta} - \tfrac{1}{\lambda})\right] \tag{3.5}$$

Here, we have used the fact that the decay length of the plasma in the scrape-off layer is roughly equal to the decay length for impurities. The parameter δ characterizes the degree of the localization of the source and is the measure of its thickness. The parametric dependence on δ is of particular interest for our study. An increase of the parameter δ simulates the enhancement of the penetration depth of oxygen neutrals due to the cross charge exchange processes.

The solution of the equation (3.2) with the source term, given by (3.5) and satisfying the boundary conditions (3.3) reads

$$N = N_o f(x) + \left\{ \frac{\Gamma_o \lambda}{D\left[\exp(\frac{a}{\lambda}) + \exp(-\frac{a}{\lambda})\right]} - N_o \frac{\int_o^a f(x)dx}{\left[\exp(\frac{a}{\lambda}) + \exp(-\frac{a}{\lambda})\right]} \right\} x$$

$$x \left[\exp(\frac{x}{\lambda}) - \exp(-\frac{x}{\lambda})\right] \qquad (3.6)$$

$$\text{Here, } N_o = \frac{\Gamma_o \delta}{D} \qquad (3.7)$$

and

$$f(x) = \frac{(\lambda-\delta)\lambda}{2(\lambda-2\delta)\delta} \exp(-\frac{x}{\lambda}) - \frac{\lambda-\delta}{\lambda-2\delta} \exp(-\frac{\lambda-\delta}{\lambda\delta} x) -$$

$$- \frac{\lambda-\delta}{2\delta} \exp(\frac{x}{\lambda}) \qquad (3.8)$$

Formulae (3.6)-(3.8) are used as a hint in the assessment of the parametric dependences and scalings, when interpreting the results of the numerical simulations.

We start the analysis, by considering the case of the "thin" scrape-off layer (the distance from the limiter head to the wall a then being much less than the plasma decay length λ and the source thickness δ). In this case, the formula (3.6) takes the form:

$$N = N_o \left[\frac{\lambda}{2(\lambda-2\delta)} \exp(-\frac{x}{\lambda}) + \frac{1}{2} \exp(\frac{x}{\lambda}) - \frac{\lambda\,\delta}{\lambda-2\delta} \times \exp - (\frac{x}{\delta} - \frac{x}{\lambda}) \right] \qquad (3.9)$$

If the source thickness δ is much shorter than the decay length λ, then the total number of impurities exponentially increases with the gradient scale of the order of the source width. The factor in front of the exponent, which has the physical meaning of the stationary density, scales as the source width δ for a given influx. Neglecting the influence of the scrape-off layer ($\frac{1}{\lambda} = 0$), this case reduces to the case considered by Engelhardt-Feneberg [10]. If the source width δ increases, the total density of impurity ions is modified. The saturation density increases faster than in the previous case with the growing width of the source.

If the plasma decay length gets of the order of a,
then the total number of impurities increases on the length scale of the order of the plasma decay length. The saturation density is approximately one half of the latter for the previous case and proportional to the penetration depth.

The situation is changed for the "thick" scrape-off layer ($a \gg \lambda, \delta$):

$$N = N_o \left[\frac{(\lambda-\delta)\lambda}{2(\lambda-2\delta)\delta} \exp(-\frac{x}{\lambda}) - \frac{(\lambda-\delta)}{(\lambda-2\delta)} \exp - (\frac{\lambda-\delta}{\lambda\delta}x) \right] \qquad (3.10)$$

If $\lambda > \delta$, the profile of the total density increases to its maximum value on the length scale of the order of the source width δ and then decreases

on the longer distance of the order of the decay length. The maximum value of the total density is almost proportional to the decay length and is weakly dependent on the source width.

4. Results and discussions.

From the equations (2.2) and (2.3) it follows that the cross charge exchange processes affect both the oxygen neutrals and the singly ionized oxygen ions if their mean free paths for charge exchange are of the same order of magnitude as the ionization mean free paths. For singly ionized oxygen ions this implies that they are not immediately depleted by the electron impact to the next ionization state, but exercise charge exchange with neutral hydrogen. To be in this regime the following local estimate are obtained for the neutral hydrogen density: $n_H \tilde{=} 0.1\ n_e$ for T = 10 eV and $n_H \tilde{=} 10^{-4}\ n_e$ for T = 3 eV. If this condition is satisfied, the term arising from the charge exchange implies a significant effect on the rate equations both for the neutral oxygen and the singly ionized oxygen ion for a very wide range of the plasma parameters.

For oxygen atoms injected with an initial energy much less than the plasma temperature, the multiple charge exchange processes produce fast oxygen neutrals with an average energy of the order of the plasma temperature and at the same time retard their directed motion by randomizing their velocity distribution. Some of the oxygen atoms (roughly one half for plasma temperatures of the order 3 eV) return to the wall reducing the net inflow of the injected impurities. The rest, moving into the plasma, penetrate much deeper owing to the increased velocity and reach the region with the higher temperature, where the ionization to the second ionization state increases drastically and the amount of the neutral hydrogen decreases.

The charge exchange processes with hydrogen affects not only the oxygen neutrals, but also the appearant diffusion of the singly ionized oxygen ions. Namely, the singly ionized oxygen ion might lose its charge by exchanging it with the neutral hydrogen, move much faster as a neutral and then get the charge back before arriving at the wall. The singly ionized oxygen ions diffuse much faster to the wall as a result of the multiple charge exchange and thus undergo greater recycling. This scheme implies an increase of the effective diffusion coefficient of the singly ionized oxygen ions as described in [7].

To demonstrate some of the typical examples of the I-D multispecies non-corona impurity transport code, some steady-state radial density profiles for oxygen are given for plasma temperature and density profiles, similar to those of the ohmically heated ASDEX plasma. Typical tokamak electron

temperature and density profiles are shown in Fig. 1.

The profiles of the total number of oxygen ions and their distributions over the ionization states are shown in Fig. 2 for the neutral hydrogen flux, varying between $\Gamma_H = 0$ and $\Gamma_H = 10^{19}$ $cm^2 s^{-1}$. Here, parallel transport in the scrape-off layer was switched off. It should be noted here that the latter value is the product of the local neutral hydrogen density and the local density of the singly charged oxygen ions, averaged over the recycling area divided by the density of the 0^+, averaged over the same area. It might appear excessive compared with the typical value averaged over the flux surfaces. However due to the significant poloidal and toroidal assymetries observed in the outer regions of the tokamak plasma, this value, corresponding to $n_H \approx n_e$, can locally assume the right order of magnitude [11]. This is certainly true for the regions with the large content of the neutral hydrogen, such as the area in the close vicinity of the limiter's top or the gas inlet, where oxygen is sputted by hydrogen neutrals. It is seen from Fig. 2, that for the constant oxygen flux the total amount of oxygen ions is increased by almost one order of magnitude due to the drastically increased penetration depth. Significant modifications also appear in the distribution of the oxygen ions over the ionization states. The low ionization states are usually located at the periphery and are therefore strongly influenced by the cross-charge exchange processes. Owing to the enhanced diffus ion, the amount of the very low ionization states(OII-OV) decreases (see formula 3.7), and their profiles get much flatter. On the other hand the relative amount of oxygen in the higher ionization states increases, leading to enhanced radiative efficiency.

The dependence of the total amount of impurities on the neutral hydrogen flux is shown in Fig.3 for the different values of the plasma temperature at the wall and the decay length in the scrape-off. It is seen that the total amount of oxygen ions scales more slowly than the penetration depth of the impurity neutrals (see formula 3.9) due to the increased albedo of the plasma for a given impurity inflow. In the formula (3.7) the influx is effectively decreased due to the increased reflectivity of the plasma.

The obvious effect of the decreasing decay length in the scrape-off is the decrease of the total amount of oxygen ions (see Fig.3). The effect of the cross charge exchange gets less important with the decreasing value of the decay length, owing to the more rapid loss of the OII. The decay length in the scrape-off layer is expected to be generally shorter for a limiter than for divertor discharges, so it is concluded that the charge-exchange process with hydrogen should affect divertor discharges more strongly than limiter discharges.

As it is seen from Fig.3, the effect of the cross-charge exchange is a very strong function of the plasma temperature at the first wall, owing to the very drastic dependence of ionization cross sections in the temperature range from 3 eV to 10 eV. In both cases it was assumed that oxygen neutrals were injected with thermal velocity corresponding to room temperature.

The dependence of the total number of oxygen ions on the injection velocity is shown in Fig. 4. It is seen that it is almost linear for the injection velocity varying from T=0.02 eV to T=0.5 eV. The dependence is also only weakly dependent on the hydrogen flux. On the other hand, the suggestion put forward in [6] that the effect of the cross charge exchange can be simulated by varying the injection velocity of the neutral oxygen atom seems questionable when Figs. 2 and 4 are compared. The main reason for this is that the cross charge exchange processes create the high energetic component deeper into the plasma and thus influence the total amount of oxygen ions stronger.

As far as molecules are concerned, the drastically increased penetration depth of the oxygen impurities is the result of the low energy chemical processes occurring to the oxygen molecular compounds, released from the wall. For the case of ASDEX it reaches the value of up to 5-10 cm. The profile of the total number of impurity ions is shown in Fig.5 for the density of the oxygen molecules, being $10^{11}\ cm^{-3}$ and for the energy 0.03 eV at the wall. Their effect is qualitatively similar to the effect of the cross charge exchange, leading to increased penetration of the neutral component produced isotropically via dissociation and heated up by the plasma. The quantitative difference is that they penetrate slightly deeper and have no effect on the transport of the low ionization states.

However, interesting physical effects arise when impurities are injected partly as molecular compounds. This case is shown in Fig.6. Comparing Fig. 5 with Fig. 6 it is seen that the total amount of oxygen penetrating into the plasma is increased by approximately 25%. It seems consistent with the simple physical model, that the oxygen atoms, launched after dissociation of molecular compounds back towards the wall are attenuated essentially only as a result of the charge-exchange with hydrogen. On the other hand, the penetration of a component moving into the plasma is very slightly influenced by the cross charge exchange processes.

The following major conclusions are drawn from the calculations: the effect of the cross charge exchange processes between oxygen and hydrogen leads to the significant increase of the total impurity content in the plasma core primarily due to the enhanced penetration of the oxygen neutrals. It is pointed out that the cross charge exchange processes result in a larger amount of oxygen neutrals returned to the wall, and a smaller amount penetrating the plasma. However, those that do penetrate, move much deeper into the core. The same mechanism is an important channel for the loss of the singly ionized oxygen ions and might play an important role, as an additional sink in the vicinity of the top of the limiter. It also implies the significant increase of the diffusion coefficient of the low ionization states of oxygen.

The combination of this effect with the fact that oxygen is partly desorbed from the metallic surfaces as molecular compounds result in the increase of the impurity content by $\sim$ 25%. The penetration depth, however, is almost unchanged.

Acknowledgements.

The authors wish to thank Prof. B. Lehnert and Dr. K. Lackner for discussions.

This work was supported by the European Communities under an association contract between Euratom and Sweden.

References.

[1] A. Gibson, M.L. Watkins in Controlled Fusion and Plasma Physics (Proc. 9th European Conf. Prague)1(1973)31.

[2] K. Lackner, J. Neuhauser, IAEA Technical Committee Meeting on Divertors and Impurity Control,eds. M. Keilhacker and U. Daybelge, 1981, Garching, FRG, p. 58.

[3] H. Furth. in Fusion (Ed. by Teller) Vol. 1, Magnetic Confinement, Part A, Academic Press, New York (1981)p. 123.

[4] K. Lackner et al. Zeit. für Naturforsch. 37a, 931, 1982.

[5] W. Langer. Nucl.Fus. 22, 751, 1982.

[6] R. Hawryluk, S. Suckewer, S.P. Hirschman. Nucl, Fus. 19. 607,1979.

[7] M. Tendler, Pl.Ph., 25, 767, 1983.

[8] D. Manos, Topical Conference on the Atomic Processes in High Temperature Plasmas, Princeton, 1983, paper D.26.

[9] K. Behringer, W. Engelhardt and G.Fussmann, IAEA Technical Committee Meeting on Divertor and Impurity Control, Garching, 1981 ed. M. Keilhacker and U. Daybelge, p. I.C.6.

[10] W. Engelhardt, W. Feneberg, Nucl. Math. 76, 518, 1978.

[11] S. Allen et al., Nucl.Fus. 21, 251, 1981.

Figure Captions.

Figure 1. Temperature and density profiles for the ohmically heated ASDEX tokamak, corresponding to a wall temperature of 10 eV and density $1x10^{12} cm^{-3}$ at the limiter location r=40 cm.

Figure 2. Profiles of the total density of the oxygen ions and some of the ionization states for oxygen flux $\Gamma_o=10^{15} cm^{-2}s^{-1}$, Solid, dashed, dotted and dash-dotted lines correspond to hydrogen flux, equal to $\Gamma_H=10^{19}$, 10^{18}, 10^{17}, $0(cm^{-2}s^{-1})$, respectively. The scrape-off layer is switched off. The temperature and density profiles are shown in Fig.1. The ionization state numbers are shown by Roman numerals.

Figure 3. Maximum total oxygen ion density as a function of the hydrogen flux for different decay lengths λ and wall temperature T_w.

Figure 4. Total number of oxygen ions as a function of the dimensionless velocity for $\Gamma_H=0,10^{19}$ $cm^{-2}sec^{-1}$, respectively.

Figure 5. Profiles of oxygen ionization states for the density of the oxygen molecules $N_{mol}=10^{11}cm^{-3}$ and an energy 0.03 eV at the wall. The oxygen atomic flux is zero.

Figure 6. Profiles of oxygen ionization states for the same density and temperature as on Fig.5 and the hydrogen flux $\Gamma_H=10^{19}$. The oxygen atomic flux is zero.

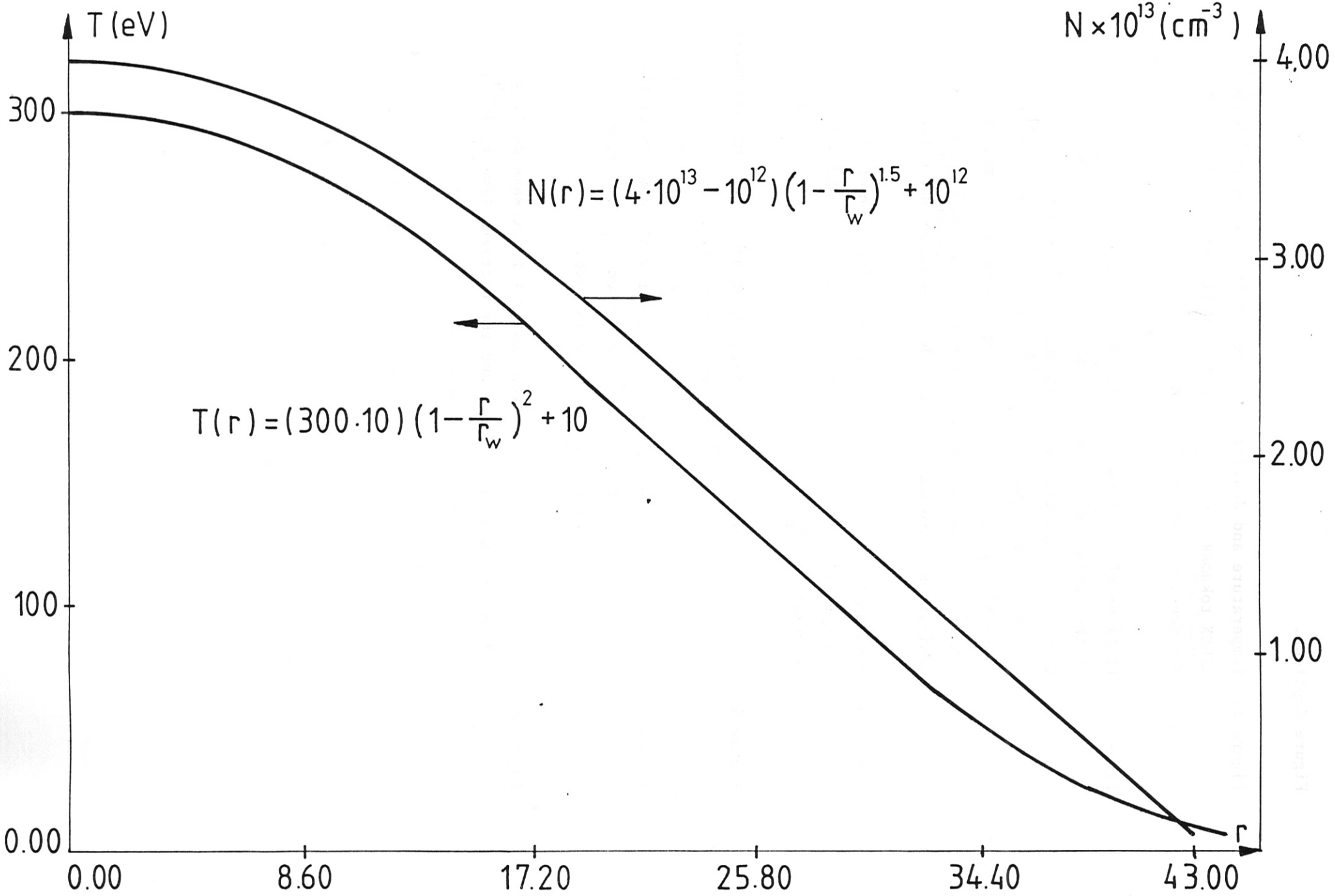
T (eV)
N × 10^13 (cm^-3)
300
200
100
0.00
4.00
3.00
2.00
1.00
0.00
8.60
17.20
25.80
34.40
43.00
r
N(r) = (4·10^13 − 10^12)(1 − r/r_w)^1.5 + 10^12
T(r) = (300·10)(1 − r/r_w)^2 + 10

Fig.1

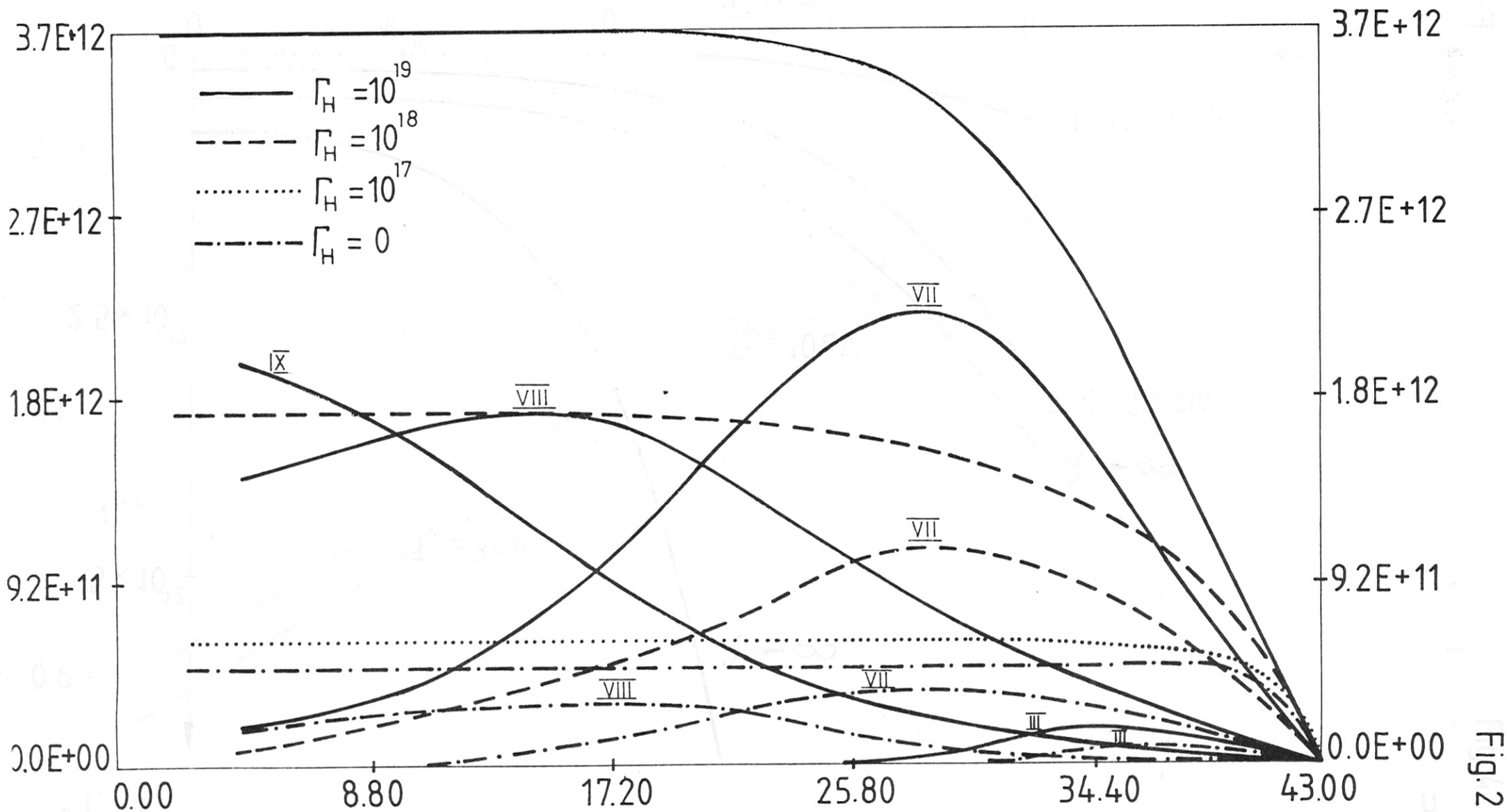
3.7E+12
2.7E+12
1.8E+12
9.2E+11
0.0E+00
$\Gamma_H = 10^{19}$
$\Gamma_H = 10^{18}$
$\Gamma_H = 10^{17}$
$\Gamma_H = 0$
IX
VIII
VII
VII
VIII
VII
III
III
0.00
8.80
17.20
25.80
34.40
43.00

Fig.2

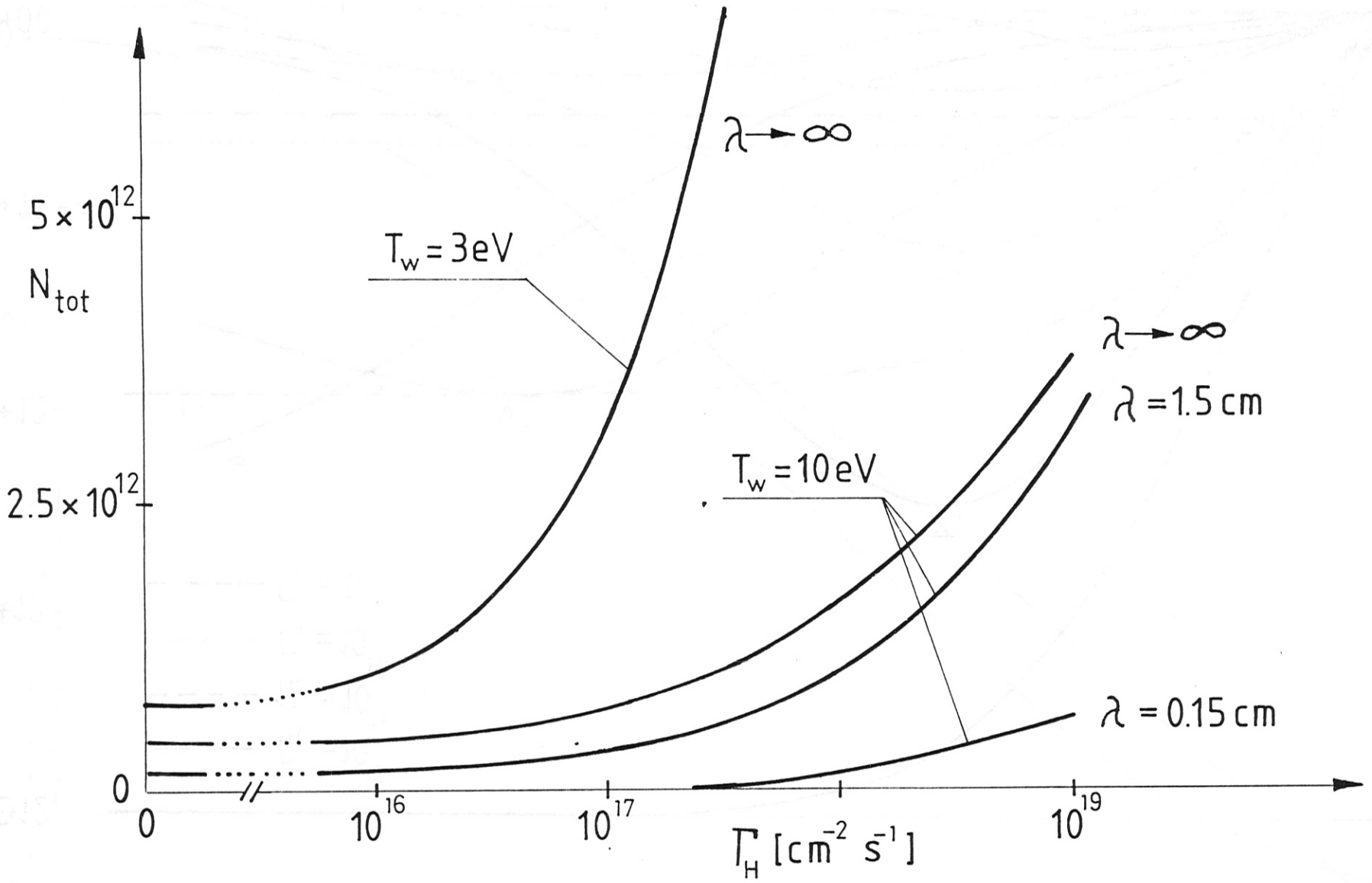
5×10^{12}
N_{tot}
2.5×10^{12}
0
0
10^{16}
10^{17}
10^{19}
Γ_H [cm^{-2} s^{-1}]
$T_w = 3$ eV
$T_w = 10$ eV
$\lambda \to \infty$
$\lambda \to \infty$
$\lambda = 1.5$ cm
$\lambda = 0.15$ cm

Fig.3

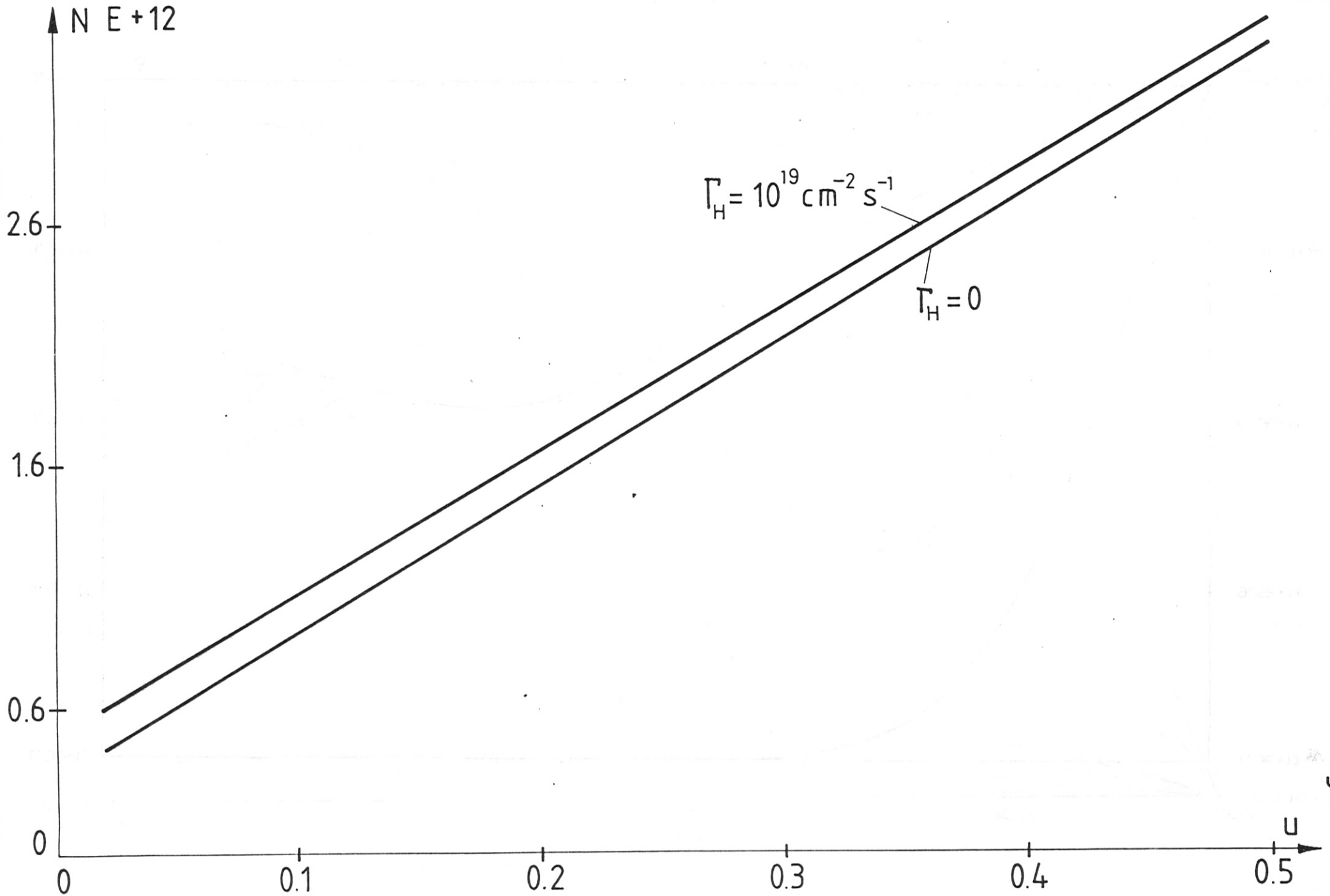

Fig. 4

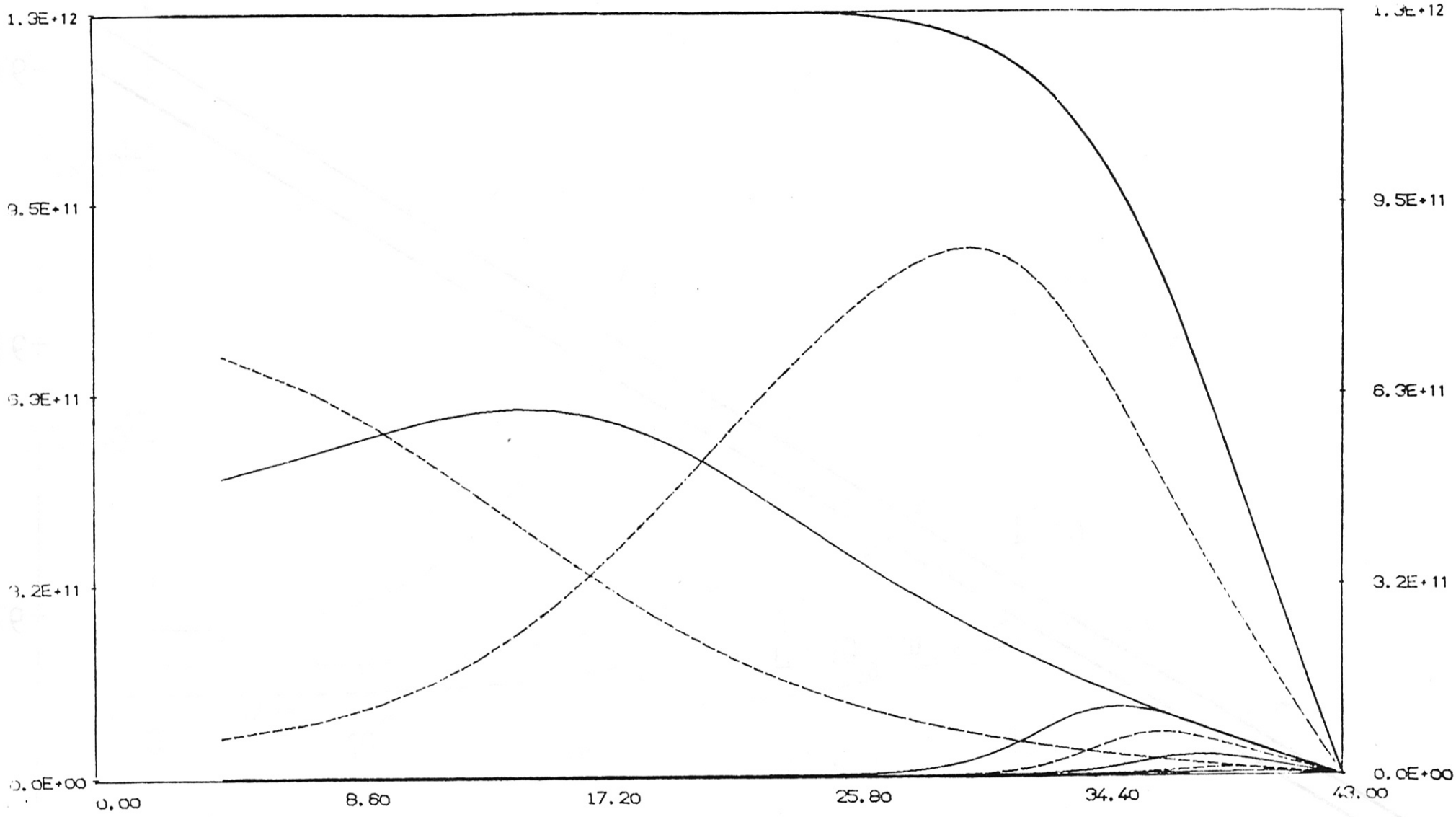

Fig. 5

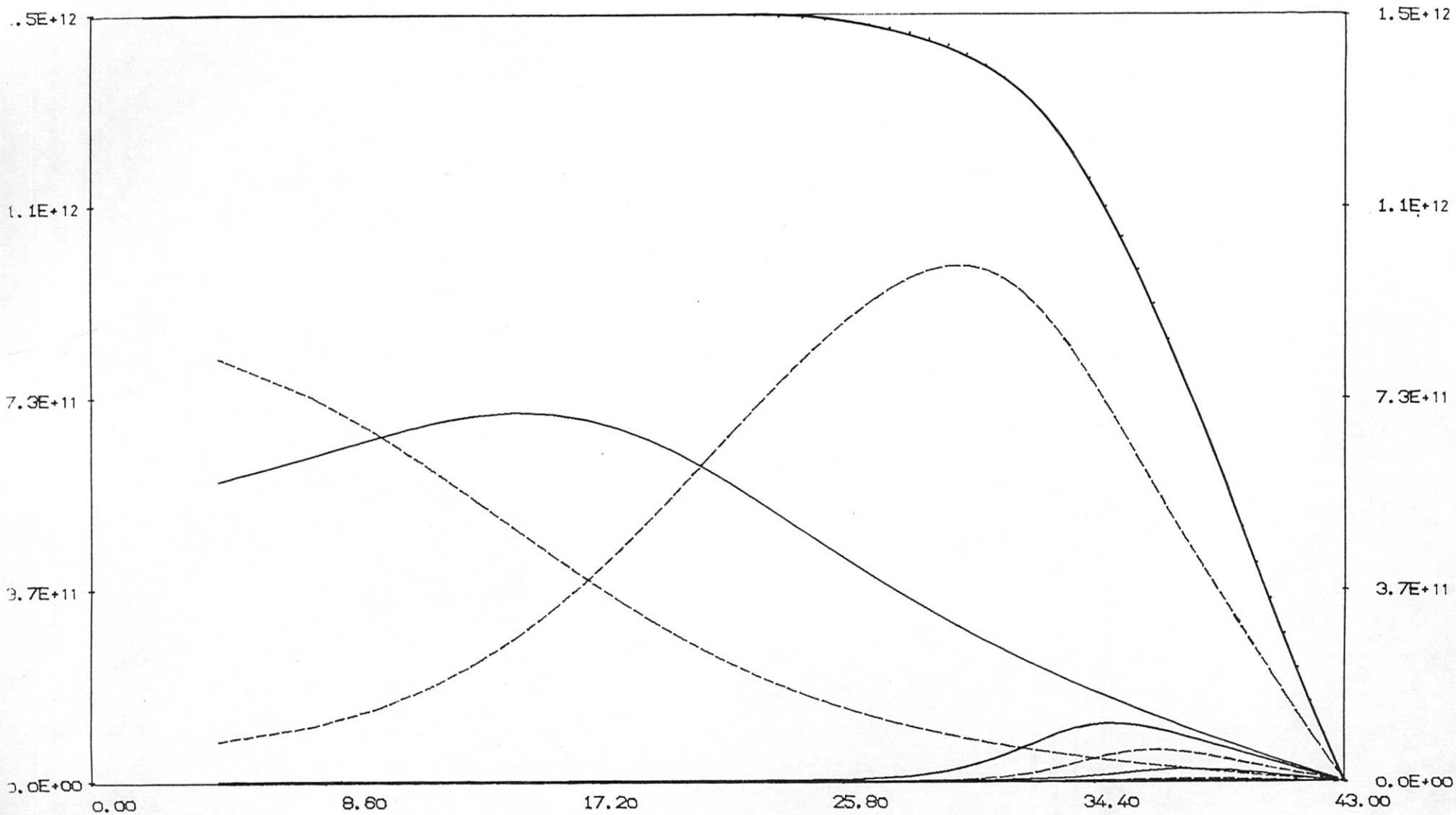
.5E+12
1.1E+12
7.3E+11
3.7E+11
0.0E+00
0.00
8.60
17.20
25.80
34.40
43.00
1.5E+12
1.1E+12
7.3E+11
3.7E+11
0.0E+00

Fig.6